Contract NAS8-31349 Code 361 (Princeton University, Princeton, NJ, 1978), pp. 60–67; D. A. Saville, *Physicochem. Hydrodyn.* **1**, 297 (1980); in *Physicochemical Hydrodynamics, V. G. Levich Festschrift*, B. D. Spaulding, Ed. (Advance Publications, London, 1977), pp. 907–910.
3. P. H. Rhodes and R. S. Snyder, in *Materials Processing in the Reduced Gravity Environment of Space*, vol. 9 of *Materials Research Society Symposia Series*, G. E. Rindone, Ed. (Elsevier, Amsterdam, 1982), pp. 225–233.
4. N. T. Dunwoody, *J. Fluid Mech.* **20**, 103 (1964); R. C. Lock, *Proc. R. Soc. London Ser. A* **233**, 105 (1955).
5. A. Kolin, D. Leenov, W. Lichten, *Biochim. Biophys. Acta* **32**, 538 (1959); A. Kolin, in *Electrokinetic Separation Methods*, P. G. Righetti *et al.*, Eds. (Elsevier/North-Holland, Amsterdam, 1979), pp. 169–172.
6. R. A. Wooding, *J. Fluid Mech.* **7**, 501 (1960); G. I. Taylor, *Z. Angew. Math. Mech.* **13**, 147 (1933).
7. The material presented in this report is based on work supported in part under NSF grant CBT-8414218.

29 April 1987; accepted 30 June 1987

X-ray Photographs of a Solar Active Region with a Multilayer Telescope at Normal Incidence

J. H. UNDERWOOD, M. E. BRUNER, B. M. HAISCH, W. A. BROWN, L. W. ACTON

An astronomical photograph was obtained with a multilayer x-ray telescope. A 4-centimeter tungsten-carbon multilayer mirror was flown as part of an experimental solar rocket payload, and successful images were taken of the sun at normal incidence at a wavelength of 44 angstroms. Coronal Si-XII emission from an active region was recorded on film; as expected, the structure is very similar to that observed at O-VIII wavelengths by the Solar Maximum Mission flat crystal spectrometer at the same time. The small, simple optical system used in this experiment appears to have achieved a resolution of 5 to 10 arc seconds.

SIGNIFICANT RECENT ADVANCES IN X-ray optics, spurred in part by new astronomical applications, include the development of thin-film, layered synthetic microstructures (multilayers) to achieve x-ray and extreme ultraviolet reflection at normal incidence (*1*). This can in principle be achieved down to a wavelength of $\lambda \approx 20$ Å, limited by the atomic dimensions of individual dielectric–spacer pair monolayers, and with reflectivity $R \approx 0.5$, over a passband, $\Delta\lambda/\lambda \approx 0.01$. This technology is of considerable interest to x-ray astronomers (*2, 3*). For a given mirror aperture a normal incidence imaging system with multilayer mirrors has an enormous advantage over grazing incidence systems in effective area and field-of-view. In addition, the surfaces are much simpler than the steep conic sections of grazing incidence optics and are therefore much easier to figure to a high degree of accuracy. Moreover, the narrowness of the passband can be used to isolate individual spectral lines and thereby make images of specific temperature regimes. Although laboratory imaging experiments have been successful in the past (*4*), to the best of our knowledge no astronomical object had been imaged with a multilayer reflector. Figure 1 is an image of a solar active region taken with a multilayer telescope.

The x-ray mirror was prepared by the Energy Conversion Devices Corporation. By means of a sputtering technique, 30 tungsten-carbon layer pairs (nominally 7.65 Å of tungsten and 14.5 Å of carbon) were deposited on a 4-cm-diameter spherical mirror having a 2-m concave radius of curvature. The mirror was designed for imaging the strong Si-XII line pair at 44.16 and 44.02 Å, slightly to the long wavelength side of the carbon K absorption edge (43.68 Å); this considerably simplified the filtering out of shorter wavelength x-ray lines. The multilayer diffraction plane-spacing was measured to be 21.93 Å on the basis of the angular reflection peak of a monochromatic beam. The mirror was designed to have a relatively broad band, hence a moderate peak reflectivity, $R \approx 0.025$. The peak wavelength of 43.86 Å met the design requirement; the absolute value of R has not yet been verified experimentally.

Figure 2 shows the Si-XII lines in relation to other solar emission features in this spectral region; the comparison spectrum was taken during a solar flare by a Lockheed rocket-borne spectrograph on 13 July 1982 (*5*). Si-XII radiation is emitted by coronal plasma at $T \approx 1.5 \times 10^6$ to 4×10^6 K, typical of active region loops, although the tail of the emissivity curve can extend to flare-like temperatures above 10^7 K (*6*). Second-order lines of O VII ($\lambda_{true} \approx 22$ Å) and third-order lines of Fe XVII ($\lambda_{true} \approx 15$ Å) are also present (dotted in the figure),

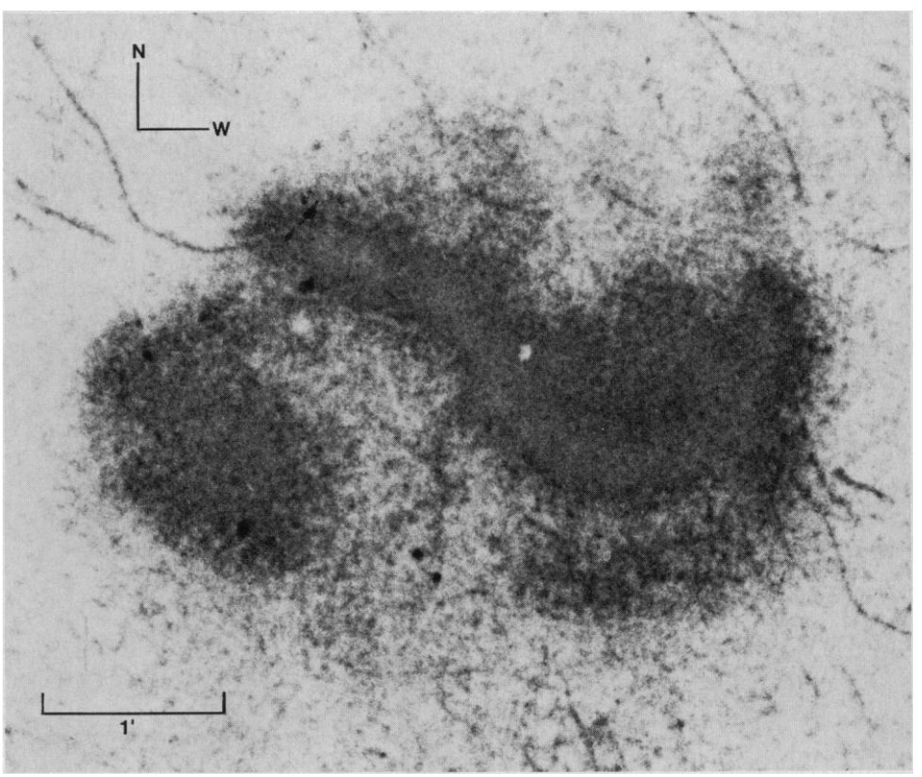

Fig. 1. A soft x-ray image of solar active region 4698/99 as imaged by a 4-cm diameter, *f*/20, multilayer telescope at a wavelength of 44 Å.

J. H. Underwood, Lawrence Berkeley Laboratory, Berkeley, CA 94720.
M. E. Bruner, B. M. Haisch, W. A. Brown, L. W. Acton, Lockheed Palo Alto Research Laboratory, Palo Alto, CA 94304.

but, because the interfaces are imperfectly sharp, the multilayer reflectivity in higher orders is smaller than the first-order reflectivity shown (~100 times reduced) so that high-order contamination is minimal. Furthermore, O-VII emissivity as a function of T is similar to that of Si XII in any event, so the plasma temperature region that is sampled remains the same.

This mirror was mounted alongside an x-ray spectrograph built in our laboratory, an ultraviolet camera from a French group, and an Hα camera, as part of an experimental solar rocket payload. The mirror was attached to the central payload spar and tilted by 1.7° to the line of sight, which allowed direct, off-axis imaging at the Herschelian focus 100 cm away, and this gave a solar image approximately 1 cm in diameter in the focal plane. The image was recorded on Kodak SO-212 film in a camera developed for an earlier rocket flight (*7*). Eight pieces of film, each with its own individual light-excluding filter, were mounted on a turret inside the camera, which was equipped with an electrically operated dark slide and shutter. The turret was rotated by a clockwork mechanism during the flight to make the exposures. The film, leftover from the Skylab mission, is sensitive to ~40- to 60-Å x-rays; it has no supercoat, and as a result the surface has become scratched over the years, somewhat degrading the quality of the image. Two polypropylene filters each of 1-μm thickness and overcoated with 1000 Å of aluminum were placed directly in front of each of the eight film pieces to exclude visible and ultraviolet light.

The Black Brant rocket that carried the payload from the White Sands Missile Range to a height of 290 km was launched on 25 October 1985 at 1720 UT. Because of a payload command link problem, only two exposures were obtained, the better of the two being the longer one (~70 seconds shown in Fig. 1) obtained on the downleg of the rocket trajectory. The only solar feature clearly visible on the film was an image of the active region complex (National Oceanic and Atmospheric Administration reference number 4698/99) at N05 W40, near the solar equator and approximately two-thirds of the way toward the west limb. This region was the only one on the visible hemisphere at the time; it had produced a class B flare at 1545 UT that, in whole sun 1 to 8 Å flux as measured by the GOES-5 satellite, exhibited a smooth decay in soft x-rays through the time of our flight. However, x-ray images from the X-ray Polychromator (XRP) on the Solar Maximum Mission (SMM) satellite demonstrated that the brightening directly associated with the flare site had largely faded by the time of our photograph.

The XRP instrument images the Sun in several x-ray lines simultaneously by rastering across a two-dimensional grid point by point, which creates a spectroheliogram with a resolution of ~15 arc seconds (*8, 9*). In Fig. 3, the overall outline of the active region obtained by the XRP in the resonance line of O VIII (Fig. 3A) (18.97 Å; $T \approx 3 \times 10^6$ K) is compared to the overall structure outlined in the multilayer photograph (Fig. 3B). We note the following: (i) The main area to the west (W region) of the x-ray emission is very similar in both; (ii) there is a definite protrusion of emission in the south of the W region in the Si-XII image, which is not seen to be detached in the O-VIII image; and (iii) the smaller area to the east (E region) is broken up in the O-VIII image, but not in the Si-XII image. By and large, the morphologies, as expected, are very similar. Optically thin, collisionally excited line emission is proportional to n_e^2 in the corona, where n_e is the electron density. At this low activity phase of the sunspot cycle the coronal plasmas elsewhere on the sun were too cool and had too low a density compared to plasma confined in active region magnetic loops to emit above our sensitivity threshold in this Si-XII–dominated passband. An x-ray spectrum covering the region from 20 to 100 Å was obtained during this flight at the far eastern side of the E region by the same spectrograph that had previously (1982) obtained the spectrum shown in Fig. 2.

A high-contrast copy of the flight film was digitized with a charge-coupled device (CCD) microdensitometer to facilitate further analysis. Digital filtering algorithms were applied, and this enhanced version of the Si-XII image is compared to the photospheric magnetic structure of the active region in Fig. 4. This magnetogram was taken at Kitt Peak Observatory earlier that day (~1425 UT). The optical alignment images from the XRP provide an accurate reference for aligning the x-ray and magnetographic images. Because the plasma producing the x-ray emission is contained by coronal magnetic fields that generally dominate the pressure balance in the corona, any features seen

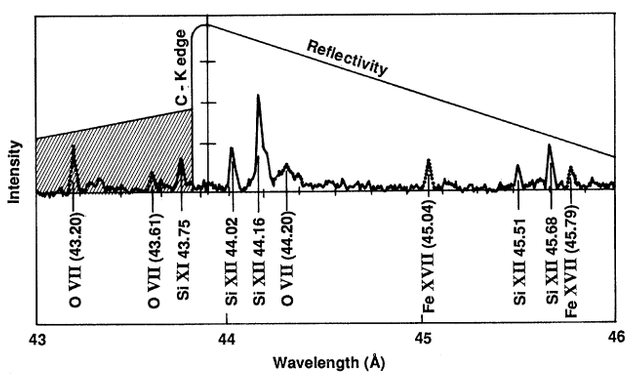

Fig. 2. The passband at ~44 Å is defined partly by the typical multilayer reflectivity profile and partly by the carbon K-absorption edge in the spacer layers and in the visible-ultraviolet polypropylene filters. The Gaussian shape of the mirror reflectivity profile is approximated by a triangle of the same half-width for convenience. In this passband the 13 July 1982 reference spectrum shows primarily Si-XII lines. The second- and third-order O-VII and Fe-XVII lines at the "equivalent wavelengths" shown (in parentheses) contribute little to the multilayer image because of the reduced reflectivity of the multilayer mirror in higher orders.

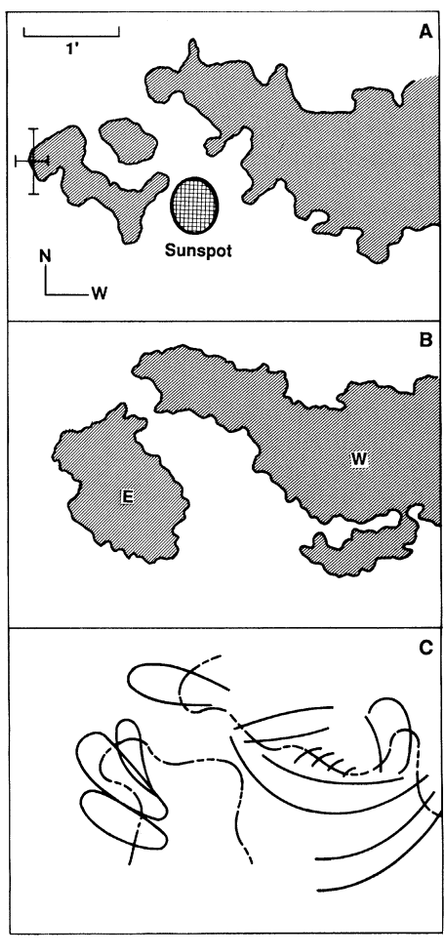

Fig. 3. (**A**) Map of O-VIII resonance radiation (18.97 Å) in the bright solar active region taken by the SMM x-ray polychromator. Error bars show the approximate location where an x-ray spectrum was taken at the edge of the E region. (**B**) Same region in Si-XII light, from image taken by the x-ray multilayer telescope. (**C**) Location of loops and neutral lines.

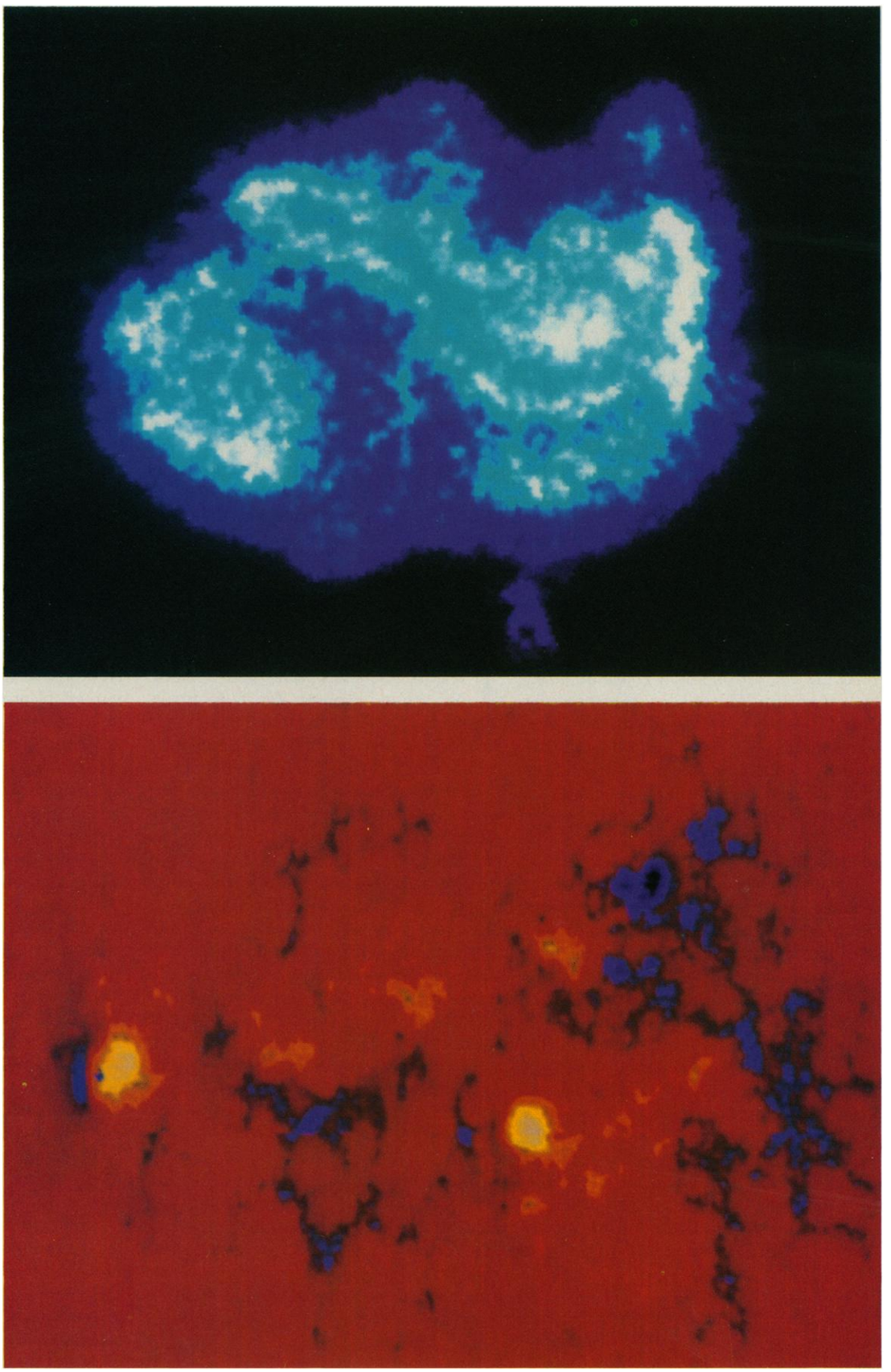

Fig. 4. (**Top**) A digitally enhanced version of Fig. 1. The photograph was digitized with a CCD system. The area outside of the active region that was solely noise was masked, obvious dust particles within the active region were removed by applying numerical interpolation, and a box filter was run over the matrix to reduce grain noise. (**Bottom**) A magnetogram of the active region to the same scale.

in the image should reflect the field structure. Preliminary analysis of the strength and shape of the differential emission measure derived from our spectrum suggests that cooling coronal loops dominate the E region; temperatures as high as $T \approx 10^7$ K are suggested, at which Si-XII emission still occurs, though with a much reduced emissivity per unit emission measure. On the basis of the magnetic topology of the W region and the fact that loops must be rooted in regions of opposite polarity, we interpret the x-ray emission therein as a combination of large-scale loops tracing out the relatively darker, predominantly E-W features, and smaller, lower-lying loops spanning the neutral line in the central part of the region where the brightness appears to peak. This qualitative interpretation is shown in Fig. 3C. Although the finest features in the image indicate an angular resolution of ~5 to 10 arc seconds, there is a diffuse quality to most of the image. Interestingly, the long sausage-like feature stretching from northeast to southwest and then curving back around to the north looks like a hollow tube. One possibility is that the core plasma is either too hot or too cool to emit Si-XII radiation strongly.

As the first astronomical image obtained by a normal incidence x-ray telescope, the image is of some interest for its own sake. The simple optical system introduced primarily two aberrations, coma and astigmatism (spherical aberration is minimal in an *f*/20 system). For a perfectly figured spherical surface optimally focused, the geometry of the optical system would have allowed for ~3 arc seconds resolution within ~12 arc minutes of the center of the field of view. The actual solar image shows linear and curvilinear features whose widths are ~23 arc seconds; the broad, linear features also show transverse brightness gradients over regions as narrow as 5 arc seconds. Despite the aberrations of this simple telescope, and the possible effect of defocusing, our postflight analysis indicates that these details of the observed structures are unlikely to be optical artifacts. Even with all the shortcomings resulting from the low-budget nature of the experiment, the ability to make this kind of photograph from a normal incidence multilayer telescope is an encouraging development for x-ray astronomy.

REFERENCES AND NOTES

1. G. F. Marshall, *Soc. Photo-Opt. Instrum. Eng. Proc.* **563** (1985).
2. J. H. Underwood, T. W. Barbee, Jr., D. C. Keith, *ibid.* **184**, 123 (1979).
3. A. V. Vinogradov and B. Ya. Zeldovich, *Appl. Opt.* **16**, 89 (1977).
4. J. H. Underwood and T. W. Barbee, Jr., *Nature (London)* **294**, 429 (1981).
5. L. W. Acton *et al.*, *Astrophys. J.* **291**, 865 (1985).
6. R. Mewe and E. H. B. M. Gronenschild, *Astron. Astrophys. Suppl. Ser.* **45**, 11 (1981).
7. J. H. Underwood and W. S. Muney, *Sol. Phys.* **1**, 129 (1967).
8. L. W. Acton *et al.*, *ibid.* **65**, 53 (1980).
9. B. M. Haisch, M. E. Bruner, M. J. Hagyard, R. M. Bonnet, *Astrophys. J.* **300**, 428 (1986).

10. We thank J. Harvey for providing the magnetogram, T. Tarbell for overseeing the microdensitometry effort, G. Joki for carrying out the laboratory mirror measurements, and K. Strong and K. Smith of the Lockheed SMM team for the XRP images. Supported in part by NASA contract NAS5-25727 and the Lockheed Independent Research Program.

15 May 1987; accepted 7 July 1987

Bat Predation and Its Influence on Calling Behavior in Neotropical Katydids

JACQUELINE J. BELWOOD AND GLENN K. MORRIS

Insectivorous bats have influenced the development of antipredator behavior in moths, green lacewings, crickets, and mantids; until recently, such adaptations were unknown in katydids. Foliage-gleaning bats in Panama can use the female-attracting, airborne calling songs of nocturnal katydids to locate prey. They also feed heavily on these insects. Katydid species sympatric with these bats exhibit markedly reduced calling song duty cycles. Males supplement shortened songs with complex, species-specific tremulations that generate vibrations that are inaudible to bats but reach conspecific females through a shared plant substrate. Female katydids do not call audibly but are also preyed on in large numbers, perhaps as a result of moving toward calling males.

IN MANY ANIMAL SPECIES, MEMBERS OF one sex use acoustic signals to attract mates (*1*). Mate-attracting calling songs are species-specific, unambiguous, and highly localizable, which helps them function successfully in sexual pair formation. These same characteristics, however, reveal the location of calling animals to predators and parasites (*2, 3*), including bats. In a study in Panama, bats responded to tape recordings of male katydids (Orthoptera: Tettigoniidae) (*4*). This report describes field and flight cage experiments with live insects to show that at least four species of tropical New World foliage-gleaning bats (FGB) (Phyllostomidae: Phyllostominae) exploit katydid songs as prey-finding cues. We show that the song duty cycle in katydids (proportion of time spent singing) is markedly reduced in species occurring in the understory of a mature forest with FGB, but not in species in secondary growth areas without these bats (*5*). We also report the occurrence of tremulation (vibration) signals in forest katydids that offset the information loss of a lowered duty cycle. These male katydids supplement their acoustic cues with complex species-specific body vibrations that are inaudible to bats, but travel through plants to conspecific females. Insectivorous bats and their prey have long coevolutionary histories, and bats have influenced the development of behavioral and morphological antipredator adaptations in moths, green lace-wings, crickets, and mantids (*6*). We present findings of widespread behavioral antibat defenses in katydids, another large group of insects.

We baited mist nets with singing male katydids to demonstrate that bats respond to song cues (*7*). Members of four FGB species (six *Micronycteris megalotis*, eight *Micronycteris hirsuta*, nine *Tonatia silvicola*, and one *Trachops cirrhosus*) responded to the calls and were caught in nets. These FGB were not attracted to control nets baited with silent females ($\chi^2 = 24$; $P < 0.001$).

Analysis of prey remains (culled, sexually dimorphic whole insect wings) that accumulate in natural FGB roosts (*8*) showed that at least one species fed heavily on katydids; 40.1% of 10,944 insects found in 12 *Micronycteris hirsuta* feeding roosts were katydids. Although they do not call, at least 50% of the katydids consumed were female. How these were located by the bats is not known.

To explore the influence of FGB predation on katydid call design, we recorded and analyzed calling songs (*9*) from 43 forest-dwelling katydid species and compared them to calls from the four dominant species who dwell in clearings. Clearing katydids signal with conspicuous calls; they have

J. J. Belwood, Entomology and Nematology Department, University of Florida, Gainesville, FL 32611, and Smithsonian Tropical Research Institute, APO Miami 34002.
G. K. Morris, Biology Department, Erindale College, University of Toronto, Mississauga, Ontario, Canada L5L 1C6.